Can an ^{18}F-ALF-NOTA-PRGD2 PET/CT Scan Predict Treatment Sensitivity to Concurrent Chemoradiotherapy in Patients with Newly Diagnosed Glioblastoma?

Hui Zhang[1,2], Ning Liu[1], Song Gao[1,2], Xudong Hu[1], Wei Zhao[1], Rongjie Tao[3], Zhaoqiu Chen[4], Jinsong Zheng[4], Xiaorong Sun[4], Liang Xu[4], Wanhu Li[4], Jinming Yu[1], and Shuanghu Yuan[1]

[1]Department of Radiation Oncology, Shandong Cancer Hospital and Institute, Jinan, Shandong, China; [2]School of Medicine and Life Sciences, University of Jinan-Shandong Academy of Medical Sciences, Jinan, Shandong, China; [3]Department of Neurosurgery, Shandong Cancer Hospital and Institute, Jinan, Shandong, China; and [4]Department of Radiology, Shandong Cancer Hospital and Institute, Jinan, Shandong, China

This study examined the value of a novel 1-step labeled integrin $\alpha_v\beta_3$–targeting ^{18}F-AlF-NOTA-PRGD2 (denoted as ^{18}F-RGD) scan in assessing sensitivity to concurrent chemoradiotherapy (CCRT) in patients with newly diagnosed glioblastoma multiforme (GBM). **Methods:** Twenty-five patients with newly diagnosed GBM were enrolled in this study 3–5 wk after surgical resection. All participants were investigated with ^{18}F-RGD PET/CT on baseline (T1) and at the third week (T2) after the start of CCRT. Tumor volume, maximal and mean standardized uptake value of the tumor (SUV_{max}, SUV_{mean}), and tumor-to-nontumor ratios of the tumor volume were obtained. The MRI treatment response was assessed at the 11th week (T3). The change in the lesion volume from T1 to T3 on MRI was used as an endpoint to evaluate the predictive ability of ^{18}F-RGD PET/CT. **Results:** With ^{18}F-RGD PET/CT imaging, we successfully visualized the residual lesions of GBM. Twenty-five and 23 ^{18}F-RGD PET/CT scans at baseline and the third week, respectively, were available for analysis. We found that ^{18}F-RGD PET/CT parameters, both pretreatment SUV_{max} on baseline ($P < 0.05$) and intratreatment SUV_{max} at the third week (SUV_{maxT2}) ($P < 0.05$) and tumor-to-nontumor ratios at the third week ($P < 0.05$), were predictive of treatment sensitivity to CCRT. Additionally, the change of volume from T1 to T2 on MRI was also predictive ($P < 0.05$). According to receiver-operating-characteristic curve analysis, the most significant parameter was SUV_{maxT2} (area under the curve, 0.846). The threshold of SUV_{maxT2} was 1.35, and its sensitivity, specificity, and accuracy were 84.6%, 90.0% and 87.0%, respectively. **Conclusion:** ^{18}F-RGD PET/CT allows for the noninvasive visualization of GBM lesions and the prediction of sensitivity to CCRT as early as 3 wk after treatment initiation.

Key Words: ^{18}F-RGD; positron emission tomography (PET); predict; chemoradiotherapy; glioblastoma

Glioblastoma multiforme (GBM) is the most common malignant primary brain tumor (*1*). Resection followed by combined radiotherapy and temozolomide chemotherapy is the standard therapy protocol for patients with GBM (*2–4*). Even with the standard therapy, the prognosis is poor, with a median overall survival of approximately 15 mo (*3,5*).

Poor prognosis of GBM is mostly attributed to its high invasiveness and frequent recurrence. Studies have shown that the recurrent lesions are mostly located in areas 2 cm from the precursor lesions (*6,7*), and recurrence in situ occurs earlier than distant metastasis. Better control of the original lesions may thus help to improve the curative effect. Identifying the nonresponders and changing the treatment plan earlier are important for effective therapy. Therefore, the early assessment of sensitivity to concurrent chemoradiotherapy (CCRT) is the premise of personalized treatment for patients with GBM.

MRI is the most important diagnostic tool for assessing brain neoplasms. Assessment of treatment efficacy of GBM is usually performed by gadolinium-enhanced MRI in 2- to 3-mo intervals during treatment (*2*). However, conventional imaging techniques usually fail to detect the effects of radio- and chemotherapy at early time points because morphologic treatment effects may be visible only after several weeks or months (*8–10*). PET allows for the assessment of tumor changes at the molecular level and may offer the possibility of detecting the tumor response to therapy at a relatively early stage (*9*). However, recent studies have demonstrated that the diagnostic accuracy of ^{18}F-FDG PET is weakened by high physiologic glucose metabolism in the brain areas in which glioma is prone to occur (*11–13*).

Various techniques have been developed to monitor the tumor response to therapy, including ^{18}F-AlF-NOTA-PRGD2 PET/CT (denoted as ^{18}F-RGD PET/CT). Arginine-glycine-aspartic acid (RGD) is a tripeptide sequence that can specifically bind to the integrin $\alpha_v\beta_3$ receptor, which plays an important role in promoting, sustaining, and regulating the angiogenesis and is expressed on tumor angiogenesis (*9,10*). It is widely accepted that the imaging of tumor angiogenesis can be used not only for the early detection of cancers but also for the monitoring of treatment outcomes (*14*). Haubner et al. (*15*) invented the first imaging agent for integrin, ^{18}F-galacto-RGD, and successfully applied it in 9 patients with good tolerance and no adverse reactions. Schnell et al. (*16*) reported the first clinical research on ^{18}F-galacto-RGD PET/CT scans in GBM patients and found that GBM demonstrated significant but heterogeneous RGD uptake, with the maximum uptake occurring in the highly proliferating and infiltrating areas of tumors, in which $\alpha_v\beta_3$

expression was prominent in tumor microvessels. Thereafter, ^{18}F-fluciclatide-RGD, ^{18}F-RGD-K5, and ^{18}F-FP-PRGD2 emerged. Studies showed that tumor uptake correlated well with the expression of integrin $\alpha_v\beta_3$. However, the radiochemical syntheses of these ^{18}F-labeled RGD tracers are complicated and time-consuming, which limits the clinical applications of this imaging agent.

In this prospective clinical study, a novel 1-step labeled integrin $\alpha_v\beta_3$–targeting PET probe, ^{18}F-AlF-NOTA-PRGD2, was used to evaluate sensitivity to CCRT in patients with newly diagnosed GBM.

MATERIALS AND METHODS

Patients

Twenty-five patients with newly diagnosed GBM and residual postoperative lesions were enrolled prospectively in this study (Table 1). There were 15 men and 10 women, with a median age of 49.5 y (age range, 30–64 y). All patients gave written consent to participate in this study, which was approved by the ethics committee of Shandong Tumor Hospital, and met the following inclusion criteria—patients had a histologically confirmed diagnosis of GBM and previously undergone surgical resection, they had MRI-based residuum postoperatively, and they were at least 18 y old and had the ability to provide written and informed consent. Further criteria included a Karnofsky performance score 70 or greater, adequate hematologic values, and sufficient hepatic and renal function. The exclusion criteria were pregnancy and inability to complete the required examinations.

Treatment

All patients were treated with radiotherapy and temozolomide 3–5 wk after surgery. In all patients, a total dose of 60 Gy was administered to the planning target volume, defined as the contrast-enhanced area from pre- and postoperative MRI including a safety margin of 2 cm and including the surrounding preoperative edema. The dose was prescribed to the reference point of the International Commission on Radiation Units and Measurements, and the fractionation was 2 Gy daily, 5 times weekly. Concurrent temozolomide was administered at 75 mg/m²/d during radiation over 6 wk, followed by a 4-wk rest phase (no temozolomide) and cycles of adjuvant temozolomide on days 1–5 of each 28-d cycle. The first adjuvant cycle was dosed at 150 mg/m²/d.

TABLE 1
Patient Characteristics

Characteristic	n
Total no.	25
Age (y)	
Median	49.5
Range	30–64
Sex	
Male	15 (60%)
Female	10 (40%)
Karnofsky performance score	80 (range, 70–90)
70–80	16
90–100	9
Pathology	GBM (World Health Organization, IV)
Surgery	Partial resection

If tolerated, subsequent cycles of adjuvant temozolomide were dosed at 200 mg/m²/d.

^{18}F-RGD PET/CT Imaging

PET/CT imaging was performed on a dedicated PET system (Discovery LS; GE Healthcare). The simple lyophilized kit for labeling the PRGD2 peptide was purchased from Jiangsu Institute of Nuclear Medicine, and the synthesis process was performed in accordance with previous studies (17). The radiochemical purity of the ^{18}F-RGD exceeded 95%, and its specific radioactivity exceeded 37 GBq (1,000 mCi)/μmol. There was no specific subject preparation, and patients did not undergo fasting and did not receive CT contrast agents. ^{18}F-RGD (224.56 ± 38.2 MBq) was injected intravenously in all patients, who were then allowed to rest for about 50 min. Scanning was performed with an integrated in-line PET/CT system (Discovery LS; GE Healthcare). PET emission images were obtained for the whole head, and the spiral CT component was performed with an x-ray tube voltage peak of 140 kV, 80 mA, a pitch of 6:1, a slice thickness of 4.25 mm, and a rotation speed of 0.8 s per rotation. A full-ring dedicated PET scan of the same axial range followed. Patients were in normal shallow respiration during image acquisition. The images were attenuation-corrected with the transmission data from CT. The attenuation-corrected PET images, CT images, and fused PET/CT images, displayed as coronal, sagittal, and transaxial slices, were viewed on a Xeleris workstation (GE Healthcare).

Image Analysis

Standard visual image interpretation was performed independently by 2 experienced nuclear medicine physicians for ^{18}F-RGD PET/CT studies with MRI as a reference. The radiotracer concentration in the regions of interest was normalized to the injected dose per kilogram of the patient's body weight to derive the SUV.

Tumor volumes (TVs) were defined as the sum of the metabolic volumes of the remaining tumors, which were derived from attenuation-corrected ^{18}F-RGD PET images. TV was obtained by including all voxels that fell within an SUV threshold determined by the SUV_{mean} of the contralateral striatum. In cases in which the tumor involved the striatum bilaterally, a threshold of 1.5 of the SUV_{mean} of the normal hemispheric background was used (18). The normal reference brain region was defined by drawing regions of interest involving the entire contralateral hemisphere at the level of the centrum semiovale (8).

MRI

All patients underwent routine MRI using a 3.0-T MRI system with pulse sequences supplied by the scanner manufacturer. Sequences including axial proton density, T1- and T2-weighted fast spin-echo images, and fluid-attenuated inversion recovery images were included. In addition, gadopentetate dimeglumine–enhanced (Magnevist; Berlex) axial and coronal T1-weighted images were acquired after contrast injection. The first MRI scan was obtained immediately before the start of CCRT (pretreatment, T1), the second MRI scan was obtained on the third week after the start of standard treatment (intratreatment, T2), and the third MRI scan was acquired 4 wk after the completion of CCRT (posttreatment, T3).

The volume of GBM lesions (VOL) was calculated simply as the lesion area multiplied by the slice thickness (19). The lesion areas were obtained by manual outlines from T1-enhanced images combined with T2 fluid-attenuated inversion recovery images of MRI. The changes of lesion volume (ΔVOL_{T1-2}, ΔVOL_{T1-3}) were calculated by $(VOL_{T2} - VOL_{T1})/VOL_{T1}$ and $(VOL_{T3} - VOL_{T1})/VOL_{T1}$.

Statistical Analysis

A statistical analysis was performed using the commercial software SPSS 17.0 (MedCalc Software) and MedCalc 11.0.1.0 (MedCalc Software Bvba, used to perform receiver-operating-characteristic [ROC] curve analysis). Twenty-five patients were classified as

responders and nonresponders according to the median value of ΔVOL_{T1-3} based on MR images. The 2-sample t test and Wilcoxon rank-sum test were used to compare the difference between the responder and nonresponder groups. Multiple clinical variables such as age, sex, and Karnofsky performance score were tested by univariate and multivariate analyses to identify the relationship between these clinical variables and the short-term outcome. The ROC curve analysis was used to obtain the threshold and determine the diagnostic accuracy of ^{18}F-RGD PET parameters in identifying responders and nonresponders.

RESULTS

Tumor Response

All 25 patients completed the entire CCRT, and 25, 24, and 25 MRI scans at T1, T2, and T3, respectively, were available for analysis. In our study, we used 2 methods to evaluate radiographic response rate. According to the Response Assessment in Neuro-Oncology (RANO) criteria, 11 patients were classified as responders (44%), including 4 complete response and 7 partial response, and 14 patients were classified as nonresponders (56%), including 10 stable disease and 4 progressive disease. According to the volume of residual lesions on MRI (Tables 2 and 3), 25 patients were classified as responders (11 patients) and nonresponders (14 patients) according to median value of ΔVOL_{T1-3} (58%).

The data obtained from the 2 methods described above are shown in Table 2.

^{18}F-RGD PET/CT Imaging Ability

With ^{18}F-RGD PET/CT imaging, the lesions of all the patients were well visualized (Fig. 1). The residual lesions of GBM had a good uptake of ^{18}F-RGD, whereas the normal brain tissue maintained a low level of uptake of the imaging probe. The high target-to-background ratios made the PET imaging contrasting. As demonstrated, along with the target lesions, the choroid plexus of the ventricle and injury to the scalp and skull inevitably exhibited good uptake of the imaging probe. However, this did not obstruct our observation of the lesions. In addition, relative to MR imaging, lesions were imaged more clearly (Fig. 2).

^{18}F-RGD PET/CT Parameters

All 25 patients completed the ^{18}F-RGD PET/CT scans at T1, and 23 completed them at T2. When the 2 groups were compared, significant differences were found in SUV_{maxT1} (the maximal SUV on baseline) and T/NT_{T1} (tumor-to-nontumor [T/NT] ratios on baseline) between responders and nonresponders. The SUV_{maxT1} of responders was lower than that of nonresponders (1.37 ± 0.40 vs. 2.14 ± 1.00, $P < 0.05$). The T/NT_{T1} of responders was also lower than that of nonresponders (17.59 ± 6.87 vs. $26, 17.11 \pm 11$, $P < 0.05$).

The difference in intratreatment parameters (such as SUV_{maxT2}, T/NT_{T2} [T/NT ratios on the third week] and TV_{T2} [tumor volume on the third week]) between the 2 groups was also statistically significant. The SUV_{maxT2}, T/NT_{T2}, and TV_{T2} of responders were lower than those of nonresponders (1.03 ± 0.39 vs. 2.19 ± 1.12, $P < 0.05$; $13.11, 9.51$ vs. 36.58 ± 25.90, $P < 0.05$; and $14,621.30 \pm 11,613.37$ vs. $34,304.00, 49164.00$, $P < 0.05$, respectively).

In addition, the change of TV (ΔTV) of the 2 groups was also different. The ΔTV of responders was higher than that of nonresponders ($-52.95\% \pm 26.80\%$ vs. $-12.93\% \pm 42.53\%$, $P < 0.05$). However, ^{18}F-RGD PET SUV_{mean} and its changes through therapy were not different between the 2 groups.

^{18}F-RGD PET/CT Parameters Compared with Other Predictors

Multiple clinical variables were tested by univariate and multivariate analyses. According to univariate analyses, baseline characteristics, such as patients' age, sex, and baseline Karnofsky performance score, did not predict short-term outcome. According to multivariate analyses, baseline characteristics considered in the multivariate models, the pretreatment parameter SUV_{maxT1} ($P < 0.05$), and the intratreatment parameters SUV_{maxT2} ($P < 0.05$) and T/NT_{T2} ($P < 0.05$) were significant predictors of CCRT sensitivity. However, the changes of TV ($P = 0.06$) and TV_{T2} ($P = 0.072$) were not predictive for short-term outcome.

Optimal ^{18}F-RGD PET/CT Criteria for Sensitivity of Chemoradiotherapy Prediction

ROC curve analysis was performed to determine the diagnostic accuracy of the 3 parameters (SUV_{maxT1}, SUV_{maxT2}, and T/NT_{T2}) in

TABLE 3
Lesion Volume Change on MRI in Patients with Newly Diagnosed Glioblastoma

Lesion volume on MRI	Average (mm³)	Range (mm³)
VOL_{T1}	27,593	6,752–67,523
VOL_{T3}	15,411	0–69,560
ΔVOL_{T1-3}	−46.85%	65% to −100%

VOL_{T1} = lesion volume on baseline of MR images; VOL_{T3} = lesion volume on 11th week of MR images; ΔVOL_{T1-3} = change ratio of lesion volume from T1 to T3.

identifying responders. By ROC curve analysis, the most significant parameter was SUV_{maxT2} (area under the curve [AUC], 0.846) (Fig. 3). The threshold of SUV_{maxT2} was 1.35, and its sensitivity, specificity, and accuracy were 84.6%, 90.0%, and 87.0%, respectively. The threshold of T/NT_{T2} (AUC, 0.785) was 19.30 and its sensitivity, specificity, and accuracy were 76.9%, 90.0%, and 82.6%, respectively. The threshold of SUV_{maxT1} (AUC, 0.737) was 1.57, and its sensitivity, specificity, and accuracy were 71.4%, 81.8%, and 76.0%, respectively.

In addition, we compared the predictive ability of ^{18}F-RGD PET/CT parameters and the volumetric parameters of MR images. Statistical analyses revealed that VOL_{T1} and VOL_{T2} were not predictive of short-term outcome ($P > 0.05$ and >0.05, respectively), but ΔVOL_{T1-2} did predict short-term outcome ($P < 0.05$). According to ROC curve analysis, the threshold of ΔVOL_{T1-2} (AUC, 0.786) was −27.68%, and its sensitivity, specificity, and accuracy were 71.4%, 80.0%, and 75.0%, respectively (Fig. 3). Consequently, by contrast, the predictive ability of ^{18}F-RGD PET SUV_{maxT2} was superior to ΔVOL_{T1-2} of MRI relative to the sensitivity to CCRT.

DISCUSSION

In this study, a novel 1-step labeled integrin $\alpha_v\beta_3$–targeting ^{18}F-RGD was used to image the residual GBM. Similar to the other approved imaging agents, ^{18}F-RGD shows excellent capability for both in vitro serum stability and in vivo tumor imaging ([14]). As for the other RGD imaging agents above, the advantage of this novel imaging agent is its simple and convenient process of radiosynthesis, which can be completed within 30 min. Its radiosynthesis improves its efficiency of imaging and clinical application. As shown in Figures 1 and 2, with ^{18}F-RGD PET/CT, lesions of GBM are well imaged with a good tumor-to-background ratio. Furthermore, both the lesions and their infiltrative area into the surrounding brain parenchyma were well imaged.

We have found that the parameters of ^{18}F-RGD PET/CT can predict sensitivity to CCRT as early as the third week when the dose of radiation reached 30 Gy. ^{18}F-RGD PET/CT intratreatment parameters, such as SUV_{maxT2} ($P < 0.05$) and T/NT_{T2} ($P < 0.05$), are prognostic of treatment sensitivity to CCRT. According to ROC curves, the most significant parameter was SUV_{maxT2} (AUC, 0.833) to predict the short-term outcome. The threshold of SUV_{maxT2} was 1.35, and its sensitivity, specificity and accuracy were 83.3%, 88.9%, and 85.7%, respectively. The threshold of T/NT_{T2} (AUC, 0.769) was 19.30, and its sensitivity, specificity, and accuracy were 75.0%, 88.9%, and 81.0%, respectively.

Moreover, ^{18}F-RGD PET/CT pretreatment parameters can also predict the short-term outcome. It identified nonresponders when the SUV_{maxT1} (AUC, 0.737) was greater than 1.57, and its sensitivity, specificity, and accuracy were 71.4%, 81.8%, and 76.0%, respectively. However, the pretreatment parameters of ^{18}F-RGD PET/CT are not as valuable as intratreatment parameters. In addition, we compared the predictive ability of ^{18}F-RGD PET/CT parameters and the volumetric parameters on MRI. By ROC curve analysis, the predictive ability of ^{18}F-RGD PET/CT parameters were superior to the volumetric parameters of MRI.

Why can the SUV_{maxT2} reflect sensitivity to CCRT? Recent work suggests that integrin $\alpha_v\beta_3$ is expressed at high levels on the surface of both glioma cells and endothelial cells of angiogenesis ([20]). The expression of $\alpha_v\beta_3$ on tumors is related to its proliferative and metastatic properties ([21,22]). GBM cells can differentiate into endothelial cells and pericytes, thus providing a means of tumor vascularization ([23]). Angiogenesis (the formation of new blood vessels from existing ones) is a vital process in the progression of GBM and is responsible for the growth of tumors. Therefore, angiogenesis imaging with RGD PET may reflect the treatment sensitivity of GBM. When CCRT is attributed to the tumor, angiogenesis shrink may be before tumor cell death and the amount of $\alpha_v\beta_3$ will drop before tumor shrinkage. Thereby, to some extent, the value of SUV on RGD PET may reflect the sensitivity to concurrent CCRT.

Why was it that the intratreatment parameters at the T2 time point were more precise than those at T1? In our study, all participants underwent partial surgical resection. As a consequence, the postoperative repair of normal brain tissues followed by extensive angiogenesis made the expression of $\alpha_v\beta_3$ upregulated at baseline (3–5 wk after surgical resection). The upregulated expression of $\alpha_v\beta_3$ of injured normal brain tissues induced by surgical resection made the pretreatment PET parameters of the operation area and residual lesion complicated. At the third week of treatment, the influence of repair following resection was weakened. ^{18}F-RGD
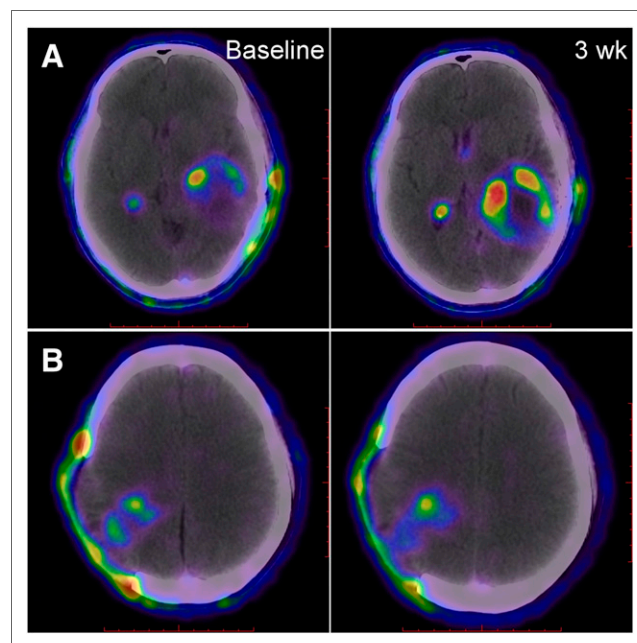
FIGURE 1. ^{18}F-RGD PET/CT at baseline and 3 wk in nonresponding patient (A; patient 11; Table 2) and responding patient (B; patient 14; Table 2).
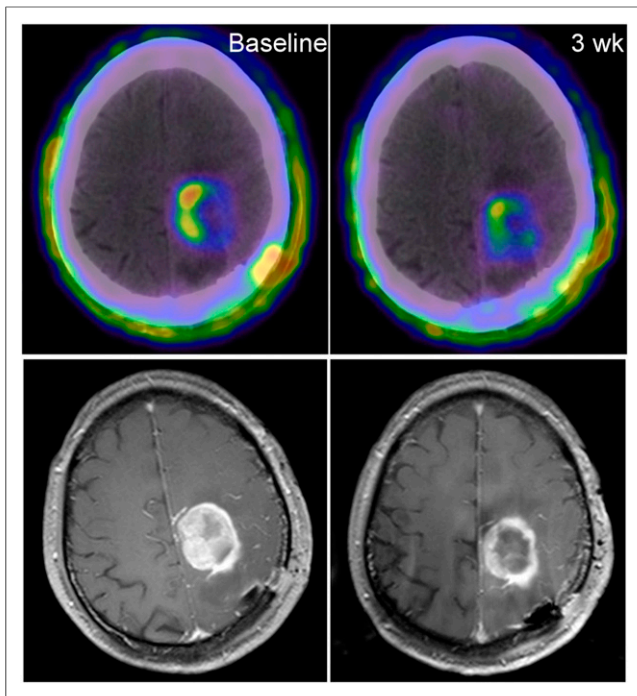
FIGURE 2. Comparison of ^{18}F-RGD PET/CT and MRI at baseline and 3 wk (patient 19; Table 2).

parameters at this time point can reflect the real level of $\alpha_v\beta_3$ expressed on cells and angiogenesis of GBM.

Additionally, several factors need to be further clarified. (1) Why was the lesion volume change determined by MRI used as the gold standard instead of RANO criteria in this study? In fact, we have correlated PET data to treatment response measured by RANO criteria, and there was no PET difference between responders and nonresponders. The results were unreasonable when inappropriate criteria were used. For example, participants 1 and 2 exhibited changes in lesion volume of −73% and −70%, respectively; however, according to the RANO criteria, they were classified as nonresponders. Participant 12 was classified as a responder but had a lesion volume that was reduced by 55%. The most important reason may be that the residual lesions after resection were characterized by cavities and irregular shapes, and the 2-dimensional measurement per RANO criteria cannot reflect the real response of GBM after CCRT. Several studies (24–26) have shown that volumetric measurement is superior to 2-dimensional measurement in evaluating the radiographic response of GBM. Wen et al. (27) believed that the use of volumetric assessment would allow for more accurate determination of the contrast-enhancing and nonenhancing volumes and overcome the limitations of 2-dimensional measurements of lesions surrounding a surgical cavity. Therefore, in our study, we chose the change of lesion volume as the evaluation criteria. (2) Contrary to other studies (8,28), it seems that all changes in ^{18}F-RGD parameters (ΔSUV$_{max}$, ΔT/NT, and ΔTV) have no close relationship to short-term outcome in this study. Perhaps this mostly depends on the influence from baseline parameters. For example, according to ΔSUV$_{max}$ = (SUV$_{maxT2}$ − SUV$_{maxT1}$)/SUV$_{maxT1}$, if the confounding factor of SUV$_{maxT1}$ is too large, ΔSUV$_{max}$ cannot represent the real change ratio of the 2 time points. Maybe it is more valuable for baseline and the change

of parameters to evaluate the treatment response of patients who have not undergone surgical resection. (3) Is there any inflammatory reaction at the intratreatment phase and will this affect the tracer uptake? There may be traumatic inflammation caused by operation that exists until the intratreatment phase. But the level of inflammation should keep going down from operation to the intratreatment phase. Studies (29,30) showed that inflammation increased the uptake of RGD tracer. Thereby, the inflammation influence to SUV$_{maxT2}$ is smaller than that to SUV$_{maxT1}$. (4) What is the relationship between tumor blood perfusion and tracer uptake? Lu N et al. (31) reported that higher levels of tumor angiogenesis (accordingly, the tracer uptake will be high) were accompanied by higher blood perfusion of tumor. However, the direct relationship of tumor blood perfusion and RGD tracer uptake has not yet been reported. (5) Will the local blood–brain barrier disruption affect the tracer uptake? Most GBM patients have variable regions of disruption of blood–brain barrier. Generally blood–brain barrier disruption will upregulate the tracer uptake (32,33). (6) Are there any changes of integrin $\alpha_v\beta_3$ induced by CCRT? In the current study, there was a significant SUV$_{max}$ decrease from T1 to T2 (SUV$_{maxT1}$ vs. SUV$_{maxT2}$, 1.37 ± 0.40 vs. 1.03 ± 0.40, $P < 0.05$) in the responder group, whereas there was no significant change in the nonresponder group (2.14 ± 1.00 vs. 2.19 ± 1.12, $P > 0.05$). Thereby, CCRT can lead to reduction of $\alpha_v\beta_3$ in sensitive tumors.

In conclusion, ^{18}F-RGD PET/CT can predict treatment sensitivity to CCRT in patients with newly diagnosed GBM as early as the third week after treatment initiation, and patients may have worse efficacy of CCRT with SUV$_{max}$ (the third week) higher than 1.35. This may be a great help to the adjustment of the clinical therapy scheme (34) and personalized treatment. In addition, considering the ease of preparation and good imaging qualities, ^{18}F-AlF-NOTA-PRGD2 may be a promising alternative to other RGD agents for PET imaging of integrin $\alpha_v\beta_3$ expression (14).

The limitation of this study was the small number of included patients. These results must be validated in a larger prospective study.
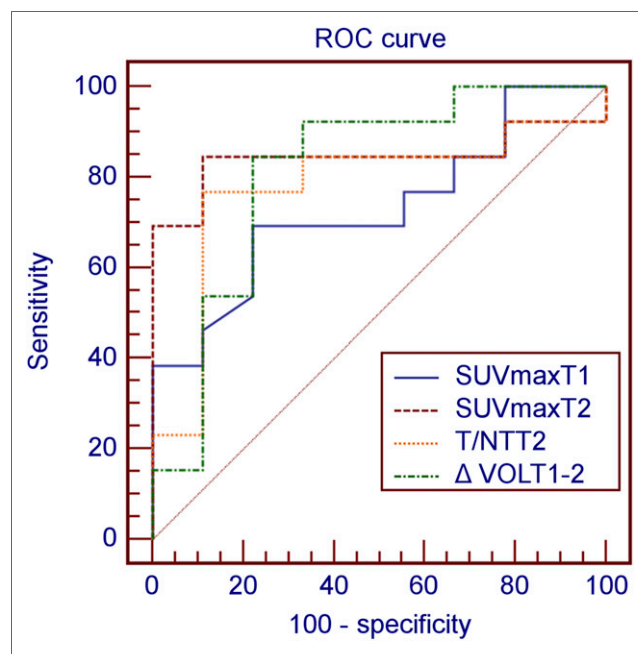
FIGURE 3. ROC curves of parameters.

CONCLUSION

This study demonstrated that PET imaging using ^{18}F-RGD allows for the noninvasive visualization of GBM lesions. Additionally, ^{18}F-RGD PET/CT provided a powerful tool to assess sensitivity to CCRT in patients with newly diagnosed GBM. In this study, the prediction of treatment response was early and time-saving, and ^{18}F-RGD PET/CT is appropriate for clinical use to supply valuable information. A further and larger validation study is needed to test the potential of ^{18}F-RGD PET/CT in guiding treatment decisions.

DISCLOSURE

REFERENCES

1. Dolecek TA, Propp JM, Stroup NE, Kruchko C. CBTRUS statistical report: primary brain and central nervous system tumors diagnosed in the United States in 2005-2009. *Neuro-oncol.* 2012;14(suppl 5):v1–v49.
2. Weller M. Novel diagnostic and therapeutic approaches to malignant glioma. *Swiss Med Wkly.* 2011;141:w13210.
3. Silber JR, Bobola MS, Blank A, Chamberlain MC. *O*(6)-methylguanine-DNA methyltransferase in glioma therapy: promise and problems. *Biochim Biophys Acta.* 2012;1826:71–82.
4. Oike T, Suzuki Y, Sugawara K, et al. Radiotherapy plus concomitant adjuvant temozolomide for glioblastoma: Japanese mono-institutional results. *PLoS One.* 2013;8:e78943.
5. Stupp R, Hegi ME, Mason WP, et al. Effects of radiotherapy with concomitant and adjuvant temozolomide versus radiotherapy alone on survival in glioblastoma in a randomised phase III study: 5-year analysis of the EORTC-NCIC trial. *Lancet Oncol.* 2009;10:459–466.
6. Milano MT, Okunieff P, Donatello RS, et al. Patterns and timing of recurrence after temozolomide-based chemoradiation for glioblastoma. *Int J Radiat Oncol Biol Phys.* 2010;78:1147–1155.
7. Brandes AA, Tosoni A, Franceschi E, et al. Recurrence pattern after temozolomide concomitant with and adjuvant to radiotherapy in newly diagnosed patients with glioblastoma: correlation with MGMT promoter methylation status. *J Clin Oncol.* 2009;27:1275–1279.
8. Rueger MA, Ameli M, Li H, et al. [^{18}F]FLT PET for non-invasive monitoring of early response to gene therapy in experimental gliomas. *Mol Imaging Biol.* 2011;13:547–557.
9. de Wit MC, de Bruin HG, Eijkenboom W, Sillevis SPA, van den Bent MJ. Immediate post-radiotherapy changes in malignant glioma can mimic tumor progression. *Neurology.* 2004;63:535–537.
10. Kumar AJ, Leeds NE, Fuller GN, et al. Malignant gliomas: MR imaging spectrum of radiation therapy- and chemotherapy-induced necrosis of the brain after treatment. *Radiology.* 2000;217:377–384.
11. Chen W, Silverman DH, Delaloye S, et al. ^{18}F-FDOPA PET imaging of brain tumors: comparison study with ^{18}F-FDG PET and evaluation of diagnostic accuracy. *J Nucl Med.* 2006;47:904–911.
12. Ricci PE, Karis JP, Heiserman JE, Fram EK, Bice AN, Drayer BP. Differentiating recurrent tumor from radiation necrosis: time for re-evaluation of positron emission tomography. *AJNR.* 1998;19:407–413.
13. Olivero WC, Dulebohn SC, Lister JR. The use of PET in evaluating patients with primary brain tumours: is it useful. *J Neurol Neurosurg Psychiatry.* 1995;58:250–252.
14. Lang L, Li W, Guo N, et al. Comparison study of [^{18}F]FAl-NOTA-PRGD2, [^{18}F]FPPRGD2, and [^{68}Ga]Ga-NOTA-PRGD2 for PET imaging of U87MG tumors in mice. *Bioconjug Chem.* 2011;22:2415–2422.
15. Haubner R, Kuhnast B, Mang C, et al. [^{18}F]galacto-RGD: synthesis, radiolabeling, metabolic stability, and radiation dose estimates. *Bioconjug Chem.* 2004;15:61–69.
16. Schnell O, Krebs B, Carlsen J, et al. Imaging of integrin $\alpha_v\beta_3$ expression in patients with malignant glioma by [^{18}F] galacto-RGD positron emission tomography. *Neuro-oncol.* 2009;11:861–870.
17. Wan W, Guo N, Pan D, et al. First experience of ^{18}F-alfatide in lung cancer patients using a new lyophilized kit for rapid radiofluorination. *J Nucl Med.* 2013;54:691–698.
18. Schwarzenberg J, Czernin J, Cloughesy TF, et al. Treatment response evaluation using ^{18}F-FDOPA PET in patients with recurrent malignant glioma on bevacizumab therapy. *Clin Cancer Res.* 2014;20:3550–3559.
19. Sorensen AG, Patel S, Harmath C, et al. Comparison of diameter and perimeter methods for tumor volume calculation. *J Clin Oncol.* 2001;19:551–557.
20. Max R, Gerritsen RR, Nooijen PT, et al. Immunohistochemical analysis of integrin alpha vbeta3 expression on tumor-associated vessels of human carcinomas. *Int J Cancer.* 1997;71:320–324.
21. Zheng DQ, Woodard AS, Fornaro M, Tallini G, Languino LR. Prostatic carcinoma cell migration via $\alpha_v\beta_3$ integrin is modulated by a focal adhesion kinase pathway. *Cancer Res.* 1999;59:1655–1664.
22. Vonlaufen A, Wiedle G, Borisch B, Birrer S, Luder P, Imhof BA. Integrin $\alpha_v\beta_3$ expression in colon carcinoma correlates with survival. *Mod Pathol.* 2001;14:1126–1132.
23. Das S, Marsden PA. Angiogenesis in glioblastoma. *N Engl J Med.* 2013;369:1561–1563.
24. Kanaly CW, Mehta AI, Ding D, et al. A novel, reproducible, and objective method for volumetric magnetic resonance imaging assessment of enhancing glioblastoma. *J Neurosurg.* 2014;121:536–542.
25. Henson JW, Ulmer S, Harris GJ. Brain tumor imaging in clinical trials. *AJNR.* 2008;29:419–424.
26. Sorensen AG, Batchelor TT, Wen PY, Zhang WT, Jain RK. Response criteria for glioma. *Nat Clin Pract Oncol.* 2008;5:634–644.
27. Wen PY, Macdonald DR, Reardon DA, et al. Updated response assessment criteria for high-grade gliomas: response assessment in neuro-oncology working group. *J Clin Oncol.* 2010;28:1963–1972.
28. Usmanij EA, de Geus-Oei LF, Troost EG, et al. ^{18}F-FDG PET early response evaluation of locally advanced non-small cell lung cancer treated with concomitant chemoradiotherapy. *J Nucl Med.* 2013;54:1528–1534.
29. Wu C, Li F, Niu G, Chen X. PET imaging of inflammation biomarkers. *Theranostics.* 2013;3:448–466.
30. Gao S, Wu H, Li W, et al. A pilot study imaging integrin $\alpha v\beta 3$ with RGD PET/CT in suspected lung cancer patients. *Eur J Nucl Med Mol Imaging.* 2015; 42:2029–2037
31. Lu N, Di Y, Feng XY, et al. CT Perfusion with acetazolamide challenge in C6 gliomas and angiogenesis. *PLoS One.* 2015;10:e0121631.
32. Oberoi RK, Parrish KE, Sio TT, Mittapalli RK, Elmquist WF, Sarkaria JN. Strategies to improve delivery of anticancer drugs across the blood–brain barrier to treat glioblastoma. *Neuro-oncol.* September 10, 2015 [Epub ahead of print].
33. Wu Y, Zhang X, Xiong Z, et al. microPET imaging of glioma integrin $\alpha v\beta 3$ expression using ^{64}Cu-labeled tetrameric RGD peptide. *J Nucl Med.* 2005;46:1707–1718.
34. Tsien CI, Brown D, Normolle D, et al. Concurrent temozolomide and dose-escalated intensity-modulated radiation therapy in newly diagnosed glioblastoma. *Clin Cancer Res.* 2012;18:273–279.